J Mol Model (2011) 17:251–263
DOI 10.1007/s00894-010-0718-4

ORIGINAL PAPER

Insight into residues involved in the structure and function of the breast cancer associated protein human gamma synuclein

Panneerselvam Manivel · Jayaraman Muthukumaran · Muthu Kannan · Ramadas Krishna

Received: 11 January 2010 / Accepted: 26 March 2010 / Published online: 2 May 2010

Abstract Aberrantly expressed human gamma synuclein (SNCG) interacts with BubR1 and heat shock protein 70 (Hsp70) in late stages of breast and ovarian cancer. This interaction is essential for progression, development and survival of cancer cells. A short, synthetically designed ankyrin-repeat-containing peptide (ANK peptide) was proven to inhibit the activity of SNCG. However, the potential binding site residues of SNCG responsible for its oncogenic function have not been reported so far. The objectives of this study were to generate a three-dimensional model of SNCG and to identify the key residues involved in interaction with BubR1, ANK peptide and Hsp70. Our study is the first attempt to report the specific binding of SNCG with the TPR motif of BubR1 and the 18kDa region of Hsp70. Our findings provide novel insights into the mechanism of interaction of SNCG, and can act as a basis for the ongoing drug design and discovery process aimed at treating breast and ovarian cancer.

Keywords Human gamma synuclein · BubR1 · Hsp70 · ANK peptide · Breast cancer

Introduction

Breast and ovarian cancers are a widespread cause of cancer-related deaths in human beings. Human gamma synuclein (SNCG) is expressed abnormally in late stage (III and IV) breast and ovarian cancers [1, 2]. SNCG belongs to the synuclein family, which also includes alpha (SNCA) and beta (SNCB) synuclein. Synucleins are small, soluble and intrinsically disordered proteins expressed predominantly in neurons [3, 4].

Hypomethylation of the CpG island in the SNCG gene results in its aberrant expression; this is detected in late stage breast and ovarian tumors whereas it is not observed in the early stages of cancer [5]. This aberrant expression of SNCG prevents apoptosis of tumor cells by inhibiting the Jun N terminal kinase (JNK) pathway, and enhances their survival through activation of the extracellular regulated kinase pathway (ERK) [6]. It enhances the invasion and migration of breast and ovarian cancer cells by activating ERK and the RHO-dependent GTPase pathway [7]. In tumor cells, it promotes resistance against various microtubule inhibitors that are used as first line chemotherapeutic agents for treating breast and ovarian carcinomas. These inhibitors activate mitotic checkpoint signaling (MCS), and also induce apoptosis in tumor cells. BubR1, a mitotic check point kinase that plays a key role in the formation of mitotic checkpoint complex (MCC), is a potential cellular target of SNCG. MCC inhibits the activation of anaphase promoting complex/cyclosome [APC/C], which ensures proper segregation of chromatids during mitotic cell division. Association of BubR1 with Mad2-bound Cdc20, a co-activator of APC, is essential for the proper function of APC, and this association is disrupted in the presence of SNCG. Interaction of SNCG with BubR1 decreases the efficacy of microtubule inhibitors. The interaction of SNCG–BubR1 proteins and disruption of BubR1–Cdc20 complex formation allows for possible interaction of SNCG with the same residues of BubR1 with which Cdc20 also interacts. The N-terminal region of BubR1 (N-BubR1) shares homology with yeast Mad3. N-BubR1 was proven to

P. Manivel · J. Muthukumaran · M. Kannan · R. Krishna (✉)
Centre of Excellence in Bioinformatics, School of Life Sciences, Pondicherry University,
Puducherry 605 014, India
email: krishstrucbio@gmail.com
email: krishna.bic@pondiuni.edu.in
URL: http://www.bicpu.edu.in/personnel.htm

interact with Cdc20 and with the C-terminal region of SNCG [8–11]. The N-BubR1–SNCG interaction was disrupted by the binding of a short, synthetically designed ankyrin-repeat-containing peptide (ANK peptide) with SNCG [12] and these results confirm the fact that the same residues in the C-terminal tail region of SNCG might be involved in interaction with both BubR1 and ANK peptide.

SNCG acts as a molecular chaperone and forms a complex with Hsp70. This interaction plays an important role in effecting the high affinity binding mode of estrogen receptor α (ER-α), which helps ER-α bind estrogen and enhances progression of estrogen dependent breast cancers [13, 14]. Although SNCG was shown to interact with Hsp70, the region of Hsp70 involved in interaction with SNCG remains unknown. The C-terminal tail region of SNCA and SNCG was found to contribute to their chaperone-like activity [15], and this region of SNCA was shown to be involved in interaction with nucleotide-free Hsp70, which enhances binding of Hsp70 with other chaperones such as HOP [16]. Human (Hs) Hsp70 contains an ATP-binding and a substrate-binding domain that is further divided into two regions: an 18kDa substrate-binding region and a 10kDa region [17, 18]. The 18kDa region of Hsp70 (18kDHsp70) is involved in interaction with other chaperones and this implies that the C-terminal tail region of SNCG might possibly interact with the 18kDHsp70 region. Finally, all these findings suggest that it is the C-terminal tail region of SNCG that harbors the residues that are important for mediating its oncogenic functions.

A knowledge of the three-dimensional (3D) structure of SNCG, and information regarding functionally important residues would help in the design of potential inhibitors for SNCG but the intrinsically disordered nature of SNCG had been a major challenging factor in the process of structure determination. However, high sequence identity between SNCG and SNCA, and the availability of a 3D structure for SNCA can be exploited in predicting the structure of SNCG. Accordingly, in this study, a 3D structure for SNCG was predicted through a homology modeling technique using the NMR structure of SNCA. Although SNCG and SNCA share high sequence similarity, they differ in function. This can help us understand the key structural differences underlying the functional diversity in these proteins. In addition, the key amino acid residues involved in mediating the oncogenic functions of SNCG were also identified based on its interaction with N-BubR1, ANK peptide and 18kDHsp70.

Materials and methods

Molecular modeling

The sequences of Hs SNCG, N-BubR1 and 18kDHsp70 were assessed using Protein BLAST [19] to find similar sequences in protein databases. The 3D structures were modeled with a comparative modeling technique using the templates obtained from the protein-BLAST search. Protein structures sharing high sequence similarity with the targets were selected as the templates (Fig. 1). The NMR structure of Hs-alpha synuclein [PDB ID: 1XQ8], the crystal structure of the conserved N terminal domain of yeast (Sc) BuB1 [PDB ID: 3ESL] and the NMR structure of the brown rat 18kDa region of heat shock protein cognate 70 (Hsc70) [PDB ID: 1CKR chain A] were used for predicting the structures of Hs SNCG, N-BubR1 and 18kDHsp70, respectively. The ITASSER server [20] was used for modeling the structure of ANK peptide through a molecular threading approach. Protein sequences were aligned using the Multalin server [21] and MODELLER 9v7 [22] was used for modeling the structures. Discrete optimized protein energy (DOPE) and modeller objective function (MOF) scores of the resulting models were used to select the most reliable model. Generated models were completed and bumps were removed using the "complete structure and remove bumps" option on the WHATIF [23] server. The final models were optimized using the "optimize python" script in the MODELLER 9v7 tool. The RamPage tool [24], WHATIF server and ERRAT [25] were used to analyze the quality of the models generated.

Active site predictions

Computer atlas surface topography of proteins (CASTp) [26], the "accessible molecular surface" option in WHATIF and the AREAIMOL option in CCP4 [27] were used for the calculation of surface accessible area in the modeled structure of SNCG. Motif Scan was performed to find the functional motifs in the modeled SNCG structure. Electrostatic calculations were carried out for the SNCG structure using the DELPHI tool in the Accelrys discovery studio (DS) suite [28]. Results obtained from the above analysis were used for defining the initial docking sites for SNCG docking studies.

Protein–protein docking studies

The easy interface of the HADDOCK (high ambiguity driven protein–protein docking) server [29] was used for protein–protein interaction studies. E110 and S124 of SNCG, G99, I100 and G101 of N-BubR1, A30, L31 and I31 of the 18kDHsp70 model and all amino acids of ANK peptide was used for SNCG–BubR1, SNCG–ANK and SNCG–18kDHsp70 docking studies. From the results obtained, the amino acids of SNCG common to interactions with BubR1, ANK peptide and Hsp70 were identified. HADDOCK results were further confirmed using the Autodock V4.0 docking suite [30]. Autodock blind docking

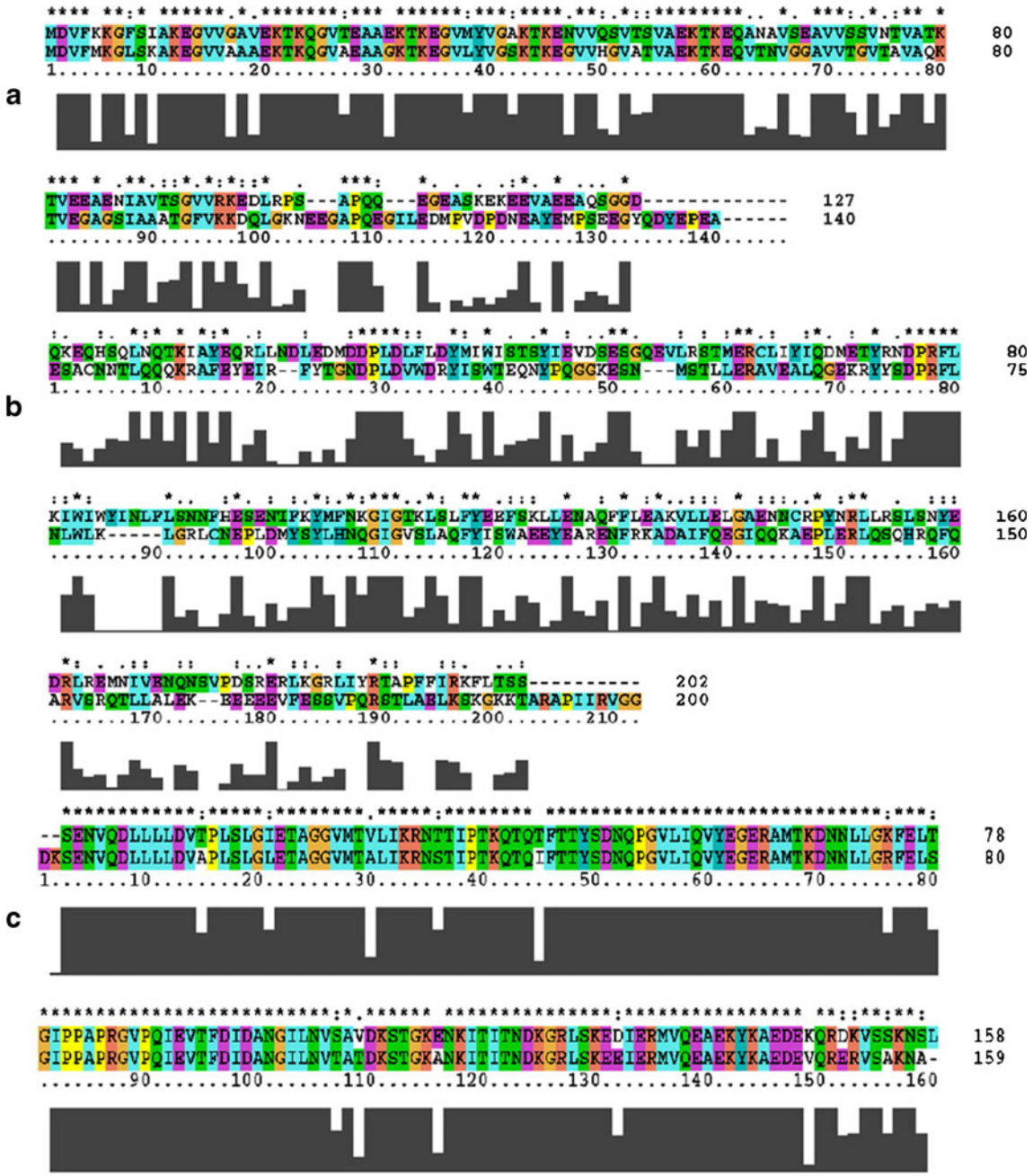

Fig. 1 Sequence alignments between **a** human gamma synuclein (SNCG) and alpha synuclein (SNCA), **b** Human N-BubR1 and yeast N-Bub1, and **c** the 18 kDa substrate-binding region of human Hsp70 and 18 kDa substrate-binding region of *Rattus norvegicus* Hsc70. *Asterisks* Single fully conserved residues, *colons* fully conserved strong groups, *periods* fully conserved weaker groups is indicated by. Sequences were aligned with ClustalX 2.0.10 [37]

methodology was employed to identify the potential amino acid residues of SNCG. For experimental convenience, the C-terminal tail region of SNCG was used for docking studies with N-BubR1, ANK peptide and 18kDHsp70, respectively. The Lamarckian genetic algorithm was used for docking simulations. For N-BubR1–SNCG protein–protein interaction studies, the C-terminal tail region of SNCG was used as the second receptor (ligand in Autodock), and N-BubR1 was used as the primary receptor (as macromolecule in Autodock). For SNCG–ANK protein–protein interactions, the C-terminal region of SNCG was kept as the primary receptor and ANK peptide was kept as the ligand structure. For 18kDHsp70–SNCG protein–protein interaction studies, the C-terminal tail region of SNCG was used as the second receptor and 18kDHsp70 was used as the primary receptor (macromolecule in Autodock). All proteins were prepared by adding Kollman charges, solvation parameters and polar hydrogens. Grid maps required for docking studies were generated using the

AutoGrid 4.0 Program supplied with AutoDock 4.0. The box sizes in the *x*-, *y*-and *z*-axis were normally set at 82 Å× 114 Å×74 Å, for N-BubR1, 88 Å×106 Å×88 Å for SNCG, and 124 Å×126 Å×106 for 18kDHsp70. The spacing between grid points was 0.64 Å for N-BubR1, 0.37 Å for SNCG and 0.56 Å for 18kDHsp70, respectively. The population size was set to 100 and individuals were initialized randomly. The maximum number of energy evaluations was set to 2,500; maximum number of generations was set to 27,000. All the AutoDock docking runs were performed using an Intel Core 2 Duo CPU at 3.0 GHz with a HP infosystem origin, with 4 GB DDR RAM. AutoDock 4.0 was compiled and run under the Microsoft Windows XP operating system. The docked poses were analyzed using DS.

Alanine scanning mutagenesis

Amino acid residues of SNCG showing interaction with N-BubR1, ANK and 18kDHsp70 were mutated to alanine and homology models were built using the Build Mutant option in DS [31]. These models were later used for docking with N-BubR1, ANK peptide and 18kDHsp70. Docking simulations were carried out as described above using AutoDock software.

Protein stability analysis

The GROMACS molecular dynamics (MD) suite [32] was used for analyzing the stability of the protein complexes. All simulations were carried out using GROMACS 4.0.7 running on a single HP windows system. The OPLS-AA force field was used. The protein complexes were solvated in a cubic box using the SPC216 water model. Periodic boundary conditions were employed to eliminate surface effects, and the 500 run of steepest descent method was used for energy minimization. All bonds were constrained using LINCS. The system was simulated at room temperature (300 K) and the Berendsen weak coupling method was used for regulating the temperature and pressure of a system. Long-range electrostatics was handled using the PME method. All potential cut-offs were set at 1.4 nm. The final MD simulations were carried out with a time-step of 1,000 ps (1 ns) and without any position restraints. All analyses were conducted using programs built within GROMACS.

Results and discussion

Molecular structure of Hs-SNCG protein

The NMR structure of Hs-SNCA is the only resource available as a starting point to understand the structure–function relationship of synuclein proteins [33]. The secondary structure architecture of these two proteins was similar and this helped us to determine the 3D structure of SNCG based on the SNCA structure. Here, the structural properties of SNCG were analyzed with reference to the SNCA structure and the differences between these two proteins were also reported. These results provide novel insights into the functional differences between these two proteins. Of the amino acid residues in the generated model, 94.4% are in the favored region (Fig. 2a). The WHATIF program predicted the RMSD Z-score of backbone–backbone contacts (0.84), backbone–sidechain contacts (−2.40), sidechain–backbone contacts (−1.81) and side-chain–sidechain contacts (−3.59). Moreover, the average structural quality control value (−1.287) is within normal range, and second generation packing quality (−1.369) values are also within the normal range, confirming the reliability of the modeled structure. In addition, the overall quality factor of the model predicted by ERRAT (74.576) was higher than that obtained for the template structure (73.016), which indicates that the predicted model is of good quality in comparison with the template (Fig. 3). Therefore, the WHATIF and ERRAT evaluation indicates that the homology modeled structure of SNCG is reasonable and reliable.

Hs SNCA and SNCG proteins have a highly conserved N-terminal region (1–85) and a less conserved C-terminal region (86–140 in SNCA and 86–127 in SNCG) and they share about 62% sequence identity.

N-terminal region

The N-terminal region of both these proteins has the 11-mer repeats characteristic of this family; six such repeats were observed in the sequences, of which the third repeat is highly conserved. These repeats share similarities with lipid binding motifs, and make up conserved apolipo-protein-like class-A2 helices. SNCG has two slightly curved helices (N and C): helix N (V3–V37) starts at the beginning of the SNCG structure, and wraps the first three 11-mer repeats, whereas the other repeats are swathed in helix C (D45–S92). These helices are arranged in antiparallel orientation, and are separated by a small linker region (M38–T44) with an unstructured coil-like topology. Unlike SNCA, the secondary structural element of (helix) SNCG does not adopt a curved architecture. Moreover, the kink introduced by residues V66 and G67 in helix C of SNCA gave a more curved appearance to this helix, whereas no such kink was seen in helix C of SNCG. In addition to this, a huge difference was also observed in the topology of linker regions in these proteins. However, despite the small differences in their structures, the N-terminal regions of these two proteins adopt similar topologies, and additionally share high sequence similarity. Furthermore, experimental

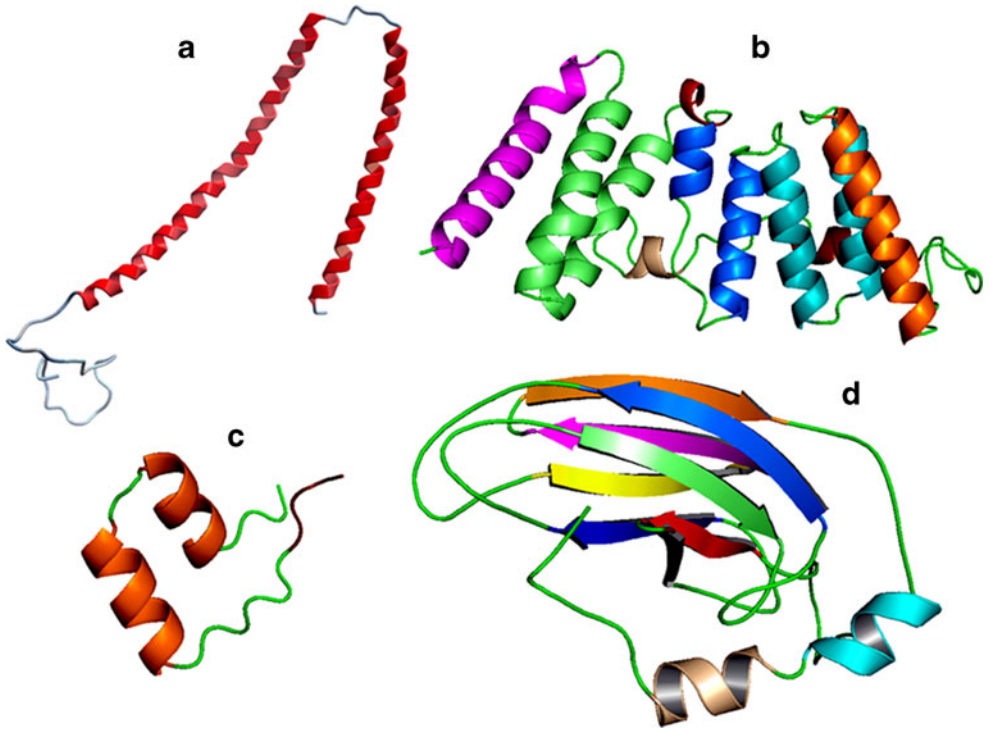

Fig. 2 **a** Cartoon representation of SNCG displaying the N-terminal helices (*red*) and C-terminal tail regions (*light gray*). **b** Cartoon representation of the human BubR1-N-terminal region displaying the first helix (*magenta*), tetratricopeptide-like fold (TPR) motif 1(helices 2&3 in *lime green*), TPR motif 2 (helices 4&5 in *blue*), TPR motif 3 (helices 6&7 in *cyan*), other helices 8 (*orange*), 9 (*dark brown*), 10 (*light brown*) and loops (*green*). **c** Cartoon representation of short ankyrin-repeat-containing (ANK) peptide showing helices (*orange*), loops (*green*) and beta turn (*brown*). **d** Cartoon representation of 18kDa region of human heat shock protein Hsp70 substrate binding domain (18kDhsp70) displaying the beta sheets (*red* L1, *dark brown* L2, *dark blue* L3, *lime green* L4, *light blue* L5, *yellow* L6, *magenta* L7, *orange* L8), helices (*cyan* H1, *light brown* H2) and loops (*green*). Figures were prepared using PyMOL molecular viewer [38]

evidence suggests that the lipid binding properties of the N-terminal regions of SNCG and SNCA are likely to be similar.

C-terminal region

Like SNCA, the terminal region of helix C (86–92) and the unstructured tail region (93–127) constitute the C-terminal region of SNCG. As discussed above, helix C shares high sequence similarity with SNCA, while a huge sequence and structural difference was observed in the tail region of these proteins. In SNCG, this region adopts a coil-like structure, whereas a long uncoiled and unstructured tail region was seen in SNCA. This tail region is rich in aspartic and glutamic acid residues, and is responsible for the flexible nature of this region. Furthermore, the tail region of both SNCA and SNCG has a chaperone-like activity similar to that of tubulin and the mitochondrial chaperonin CNP60 protein. The flexible polar tail region of these proteins was shown to interact with other proteins. Although various studies have confirmed the strong protein–protein interacting properties of this region, they have also revealed differences in the interacting partners of these proteins. Structural differences in the tail region of these proteins contribute to their functional differences. The above mentioned differences in structure cause them to deviate from each other by as much as 6.612 Å (Fig. 4a).

Identification of potential amino acid residues of SNCG involved in interaction with BubR1, ANK peptide and Hsp70 proteins

Considering the oncogenic role of SNCG, we performed molecular docking studies of SNCG with BubR1, ANK peptide and Hsp70. We first predicted the 3D structures of the Hs-N-terminal region of BubR1, the 18kDa region of substrate binding domain of Hsp70 and ANK peptide and used these models for interaction studies. Thorough analysis of these structures led to the conclusions outlined in the following sections.

3D structure of Hs-BubR1-N terminal region

Hs-BubR1 is a 120 kDa multi-domain protein. It has a conserved N-terminal region, a central non-conserved region and a C-terminal serine/threonine kinase domain. The C-terminal kinase domain is involved in the phosphory-

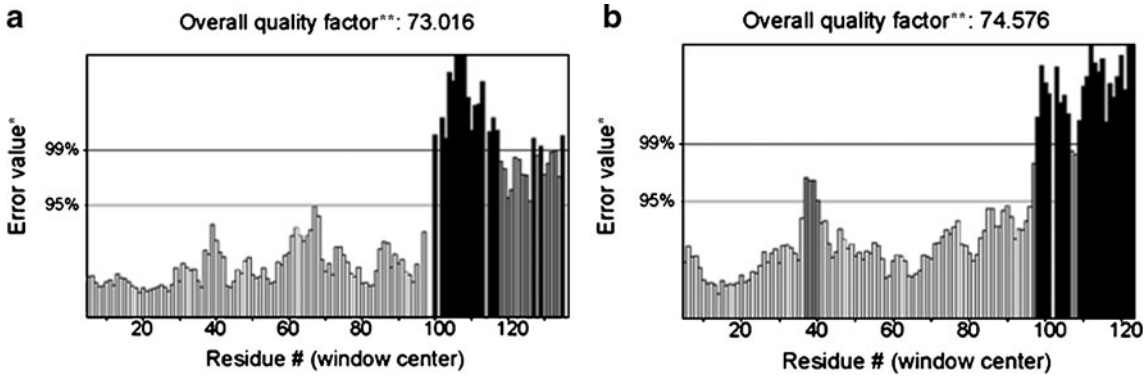

Fig. 3 Overall structural quality factor for (**a**) human SNCA and (**b**) human SNCG as evaluated by the ERRAT web server

lation of critical components of a mitotic checkpoint pathway, whereas the central region is involved in binding of other components of mitotic spindle checkpoint assembly. N-BubR1 is involved in interaction with Cdc20. Here, we predicted the structure of this region (47–247) using the crystal structure of Sc-Bub1 (PDB ID: 3ESl chain A) [34]. Despite these proteins having highly conserved N-terminal regions, yet they share only about 27% sequence identity. The sequence similarity of these two proteins was thoroughly analyzed by Bolanos-Garcia et al. [34] in studies to determine the crystal structure of yeast BUB1. The predicted structure has 96.00% of amino acid residues in the favored region, ~2.5% of residues in the allowed region, and 1.5% residues in the disallowed region. Moreover, the predicted structure has about 0.7 Å root mean square deviation (RMSD; Fig. 4b) with the crystallographic structure used.

As in Sc-Bub1, Hs-N-BubR1 also has tetratricopeptide-like folds (TPR) as shown in Fig. 2b. The structure of Hs-N-Bubr1 has ten α-helices (H1–H10), of which H2–H7 form the characteristic TPR fold repeats. Each TPR unit [TPR1 (H2–H3), TPR2 (H4–H5) and TPR3 (H6–H7)] consists of two antiparallel α helices arranged in a helix–turn–helix fashion. A short 3_{10} helix (residues K66–Y69) connects TPR1 and TPR2, whereas a short loop (I100–S103) connects TPR2 and TPR3. Like Sc-Bub1, TPR motifs of Hs-N-BubR1 also exhibit a unique arrangement of TPR motifs. This unique arrangement of TPR motifs forms a right-handed super-helical structure with a concave surface on one side and a convex surface on the other side.

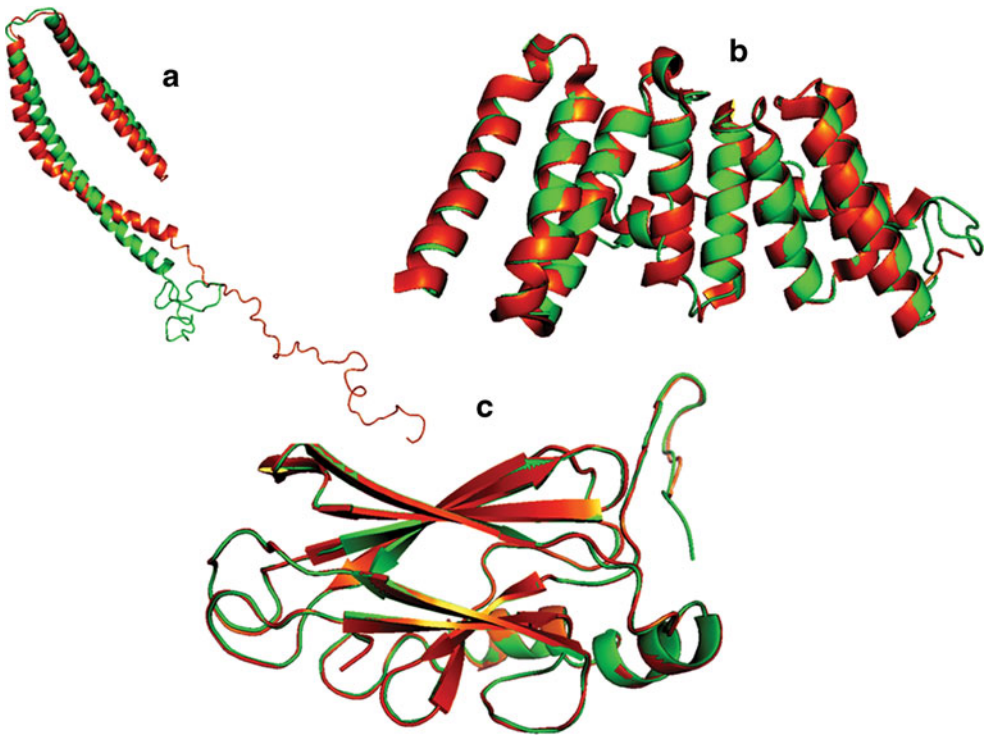

Fig. 4 Structural superimposition of **a** human SNCG with human SNCA, **b** human N-BubR1 with yeast N-Bub1 and **c** 18 kDa substrate-binding region of human Hsp70 with 18 kDa substrate-binding region of *Rattus norvegicus* Hsc70. Superimposed structures are displayed in cartoon representation: *orange* template structures, *green* proposed models. Structures were displayed, superimposed and figures were prepared using the PyMOL molecular viewer v1.1

Each TPR unit is defined by the small hydrophobic residues and large hydrophobic residues forming the interface between the TPR units. Capping helix features identified in TPR motifs of the HOP protein was also observed in helix H8 (L139–Q156). Helices H9 (S172–L180) and H10 (K189–A193) were arranged parallel to the long axis of the TPR motifs. Short loops 1(T157–E171) and 2(A181–K188) were observed between H8 and H9, and H9 and H10, respectively. Moreover, beyond H10, a short loop-like region (P194–G200) was observed in N-BubR1 but not in Bub1. Considerable structural differences between BubR1 and Bub1 were observed in the regions beyond helix H8. Both Bub1 and BubR1 have the conserved loop residues D26, Y69, D71, G99, I100, G101 and P138. Conserved GN/DD and GIG motifs of these proteins are involved in interaction with the protein Blinkin, whereas the GIG motif was found to be crucial for interactions with Cdc20 protein. This motif was also conserved in the yeast Mad3 protein, indicating its importance in the interaction with Cdc20.

3D structure of ANK peptide

Consensus repeats of 34 amino acid (aa) residues constitute the unique ankyrin protein. Ankyrin repeat proteins are found in a variety of organisms ranging from bacteria to animals, and are present in a wide variety of proteins. Each ankyrin repeat has two α-helices arranged in anti-parallel orientation connected by a short conserved loop. A β-turn precedes the helices and connects the neighboring repeats. Ankyrin proteins are characterized by their strong protein–protein interacting abilities. Each ANK repeat can establish strong binding with its target peptides. Recently, a short 34aa long ANK peptide designed by Singh et al. [12] was shown to bind strongly with the C-terminal region of SNCG, and to interrupt binding of SNCG with Hs-N-BubR1. Considering the molecular importance of this interaction, we predicted the structure of the ANK peptide using the molecular threading method. This predicted model was then used to identify the functional sites in the SNCG structure. The predicted model was in good agreement with its secondary structure, with about 90.6% of amino acid residues in the favored region and about 9.4% of residues in the allowed region of the Ramachandran plot.

Structure of ANK peptide

In the following sections, the predicted 34-aa ANK peptide (KGNSALHVASQHGHLGCIQTLVRYGANVTMQNHG; conserved residues underlined) is discussed with reference to the crystal structure of the synthetically designed ANK protein [PDB ID: 1 MJ0] [35], which has a β-turn followed by two α-helices arranged in anti-parallel orientation separated by a short loop region (Fig. 2c).

β-turn

Residues QNHG (31–34) of the modeled structure forms the β-turn structure, whereas the same structure was formed by the residues DKFG in 1 MJ0. Residues in this turn have the ability to establish hydrogen bonds (H-bonds) with their target peptides, as is evident in the observed H-bond contacts in the crystal structure.

α-helices

The conserved TPLH motif in 1 MJ0 forms the cap region of the α helix, while the cap region was formed by the residues SALH in the modeled structure. This motif is conserved throughout the family of ANK repeat proteins. Residues in this motif have the strong ability to form hydrophobic contacts with their target peptides.

Loop

Conserved residues GHLG in the modeled structure form the loop connecting the two α-helices, whilst this loop was formed by residues GHLE in 1 MJ0. Residues in this loop region form H-bond contacts with their target peptides with high efficiency.

Structure of 18kDa region of Hs-Hsp70-substrate binding domain

The substrate binding domain of Hsp70 has an 18kDa substrate binding region and a 10kDa region. The 18kDa region is involved in binding the substrate peptides, while the 10kDa region is involved in binding with other co-chaperones. Here, we modeled the structure of the 18kDa substrate binding region of Hs-Hsp70 (382–541) using the NMR structure of the 18kD region of Hsc70 from brown rat (PDB ID: 1CKR chain A) [36]. Hsp70 and Hsc70 share sequence and functional similarity with each other and this facilitated our modeling work. The 18kDa region of both proteins shares about 96% sequence identity. The predicted structure has 0.219 Å RMSD relative to the template structure (Fig. 4c), and has about 82.3% of residues in the favored region and about 12.7% of residues in the allowed region of the Ramachandran plot, while only 76.4% of residues in 1CKR were present in the favored region.

The Hsp70 substrate binding domain (Fig. 2d) has a characteristic beta domain (L19–I121) followed by a single helix C (K130–D147). Due to the presence of a kink at position Q138, helix C was represented as two helices: A (K130–V137) and B (A140–D147). This region is followed by a loop (E148–L157) that connects the terminal 10kDa region. The β-domain has four stranded anti-parallel

β-sheets stacked in a sandwich fashion, in which the top and bottom sheets are placed in an anti-parallel arrangement. The top sheets B5 (N72–L79), B4 (V56–E62), B1 (L19–T23) and B2 (G26–T29) were highly irregular, while bottom sheets B3 (T40–F46), B6 (I92–D99), B7 (G102–D110) and B8 (G114–I121) were moderately regular. Peptides bind to residues placed between loops (*L*) *L*1, *L*2 and *L*3, *L*4. These form the primary interaction loops, and are surrounded by a second set of loops: *L*4, *L5* and *L*5, *L6*.

Structural analysis of the molecular interaction of SNCG with N-BubR1, ANK peptide and 18kDHsp70-a

Accessible surface area calculations for SNCG revealed that most of the residues in the C-terminal tail are highly exposed to solvents. In particular, residues Q106, Q107, E110, K113, E114, E117, E120 and D127 show very good surface accessible properties (Fig. 5b). Moreover, these residues also possess appreciable electrostatic properties, which were apparent in the mean potentials as calculated by Delphi: −0.49 for Q106, −8.8 for Q107, −15.21 for E110, −3.3 for K113, −28.62 for E114, −9.15 for E117, 12.9 for E120 and −24.65 for D127 (Fig. 5a). Although Q106 and K113 have less electrostatic potential, they possess appreciable solvent accessibility, which favored their selection. All these results indicate that the residues in the C-terminal tail region of SNCG might have strong interacting abilities with other proteins. Calculated electrostatic properties and solvent accessibility results favored the selection of these residues for further interaction studies.

N-BubR1-SNCG interactions

Based on the docking studies, residues Q106, Q107, E108, E110, S112, K113, E114, E117, E120, S124 and D127 of the SNCG C-terminal tail region were found to have good interaction with N-BubR1 (Fig. 6a). These residues were involved in the formation of H-bonds with the residues of N-BubR1. Moreover, residues 62–189 in the BubR1-N-terminal region show high sequence similarity with region1 of Mad3, which is known to interact with Cdc20. Interestingly, amino acids in this region of N-BubR1 also show good interaction with the above mentioned residues of SNCG. This finding supports our suggestion that both Cdc20 and SNCG must interact with the same region of N-BubR1, and that the potential interacting residues of N-BubR1 must be present in the region 62–189. Furthermore, among the residues of N-BubR1 that interact with SNCG, residues K66, R67, N97, Q98, G99, K123 and E140 are highly conserved among N-BubR1 and Mad3, and also interact with Cdc20, which indicates that these residues might play an important role in mediating interaction with both SNCG and Cdc20. This region of N-BubR1 also plays an important role in interaction with Blinkin protein—a disordered protein similar to SNCG. This fact introduces the possibility that SNCG might share sequence similarity with Blinkin. Indeed, residues Q106, Q107, G109, E110,

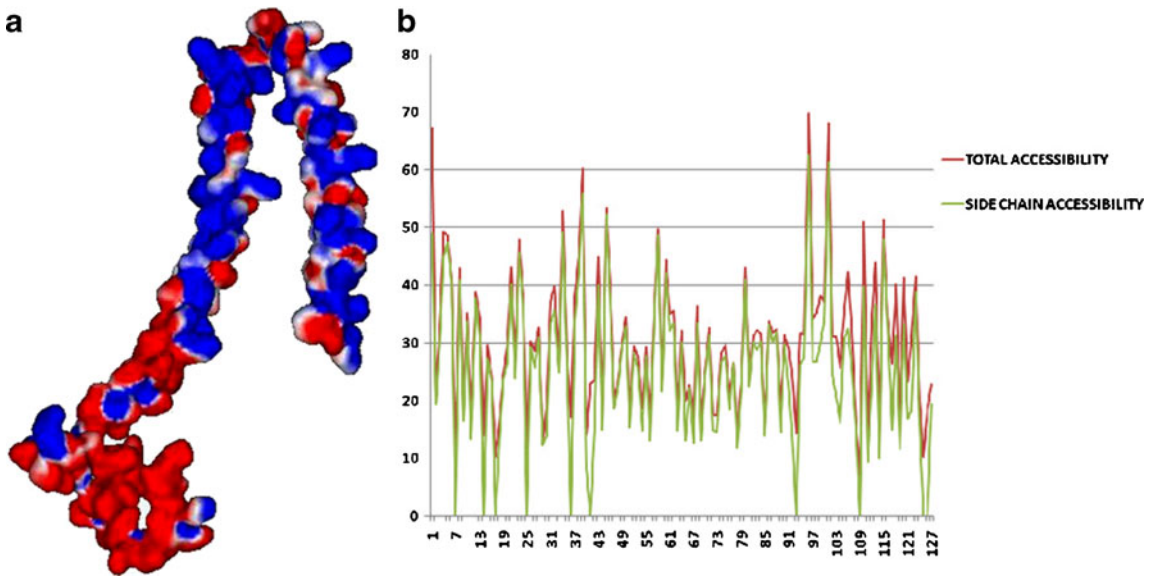

Fig. 5 **a** Electrostatic properties of SNCG residues as calculated using DELPHI tools in the Accelrys Discovery studio (DS) suite. *Red* Residues displaying very good electrostatics properties. **b** Graph displaying the surface accessible area (ASA) of SNCG. *Red* Total ASA, *green* side chain accessibility

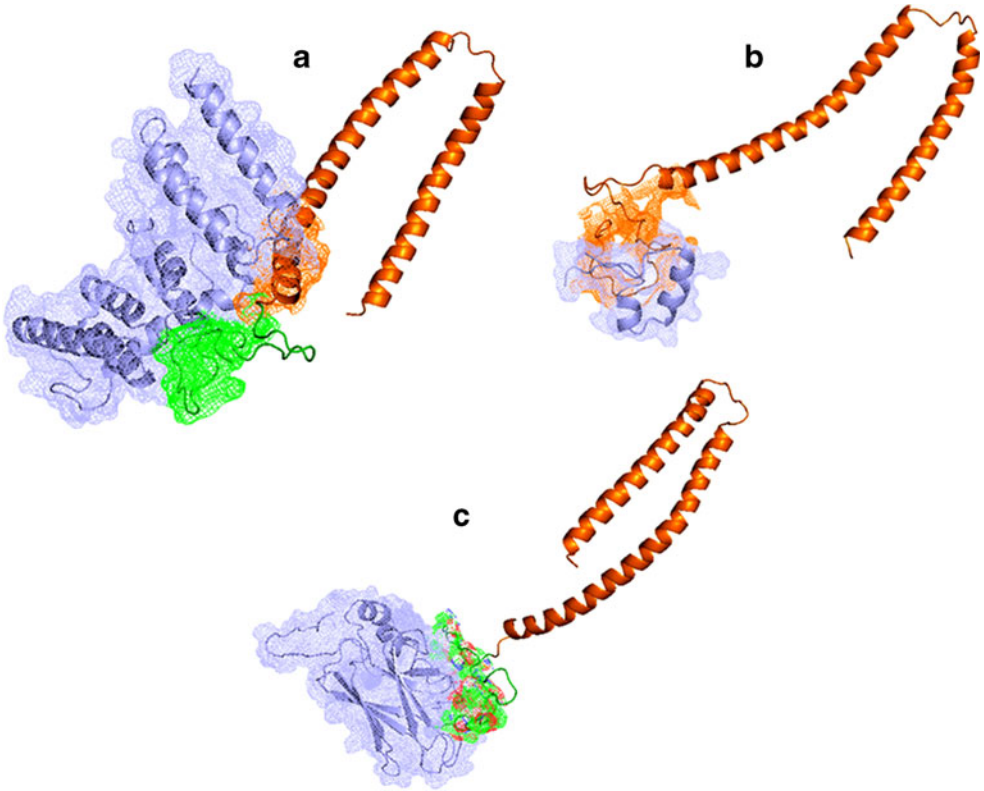

Fig. 6 **a** Interacting conformation of SNCG and N-BubR1. **b** SNCG and ANK peptide interactions. **c** SNCG-18kDHsp70 interaction. SNCG is represented in cartoon representation. N-BubR1, ANK peptide and 18KdHsp70 are represented in mesh form and their helices are represented in cartoon form (*sky-blue*)

E114, A119, G126 and D127 of SNCG were found to be shared with Blinkin. This finding suggests the possibility that SNCG could mimic the structure of Blinkin in order to interact with N-BubR1, although this hypothesis awaits experimental verification.

Finally, based on all these findings, we suggest that Q106, Q107, E108, E110, E114, E117, E120 and D127 of SNCG might play an important role in mediating its interaction with region1 of N-BubR1, which has been proven experimentally to interact with Cdc20. In addition to the above-mentioned residues, S112, A119, A124 and K113 of SNCG also show good interaction with region1 residues of N-BubR1. Both SNCG and the TPR motif of N-BubR1 share structural similarity with the 14-3-3 protein family. Furthermore, SNCA also shows similarity with the 14-3-3 protein family, and it also interacts with other members of this family. This unique property of SNCA was also observed in SNCG, which was clear from its interaction with the N-terminal TPR motif of N-BubR1. This leads to the possibility that SNCG interacts with other TPR motif-containing proteins. However, so far this has not been observed experimentally. Furthermore, in the assays carried out to analyze N-BubR1–SNCG interactions, SNCG was not observed to make any such interactions with other homologs of BubR1 such as Bub1, which also possesses TPR motifs. All these findings suggest that SNCG might have unique binding properties for the TPR motif of N-BubR1, which identifies it as a unique TPR-binding protein. Details of interacting residues of SNCG are provided in Table 1.

ANK peptide–SNCG interactions

Residues G2, L6, H7, A9, L21 and A24 of ANK peptide showed stable H-bond interactions with D127, E117, E114, and E110 of SNCG, respectively. In addition, these residues of ANK peptide are conserved throughout the family of ANK proteins. Other residues of SNCG involved in interaction with ANK peptide were Q106, Q107, E108, E117, E120 and E121. ANK peptide has been biochemically proven to interact with SNCG, and by doing so it disrupts the interaction of SNCG with N-BubR1. This fact indicates that SNCG residues targeted by ANK peptide should also be involved in interaction with N-BubR1. Accordingly, Q106, Q107, E110, E114, E117, E120 and D127 of SNCG were found to be the common residues involved in interaction with both N-BubR1 and ANK peptide. The ANK peptide–SNCG conformation is presented in Fig. 6b.

18kDHsp70–SNCG interactions

Residues D127, E120, G126, E110, Q106, E114, Q107, E108, E124, E125, D99, E98 and R96 of SNCG show good

Table 1 Residues of human gamma synuclein (SNCG) involved in interaction with the N-terminal region of BubR1 (N-BubR1), ankyrin repeat-containing short peptide (ANK), and human heat shock protein (Hsp70). Interaction energies and interacting residues were determined using the AutoDock Tool

Protein–protein interaction		Energy parameters			
		Interacting residues	Free energy of binding (ΔG) kcal/mol	vdW + Hbond + desolv energy kcal/mol	Electrostatic energy kcal/mol
N-BubR1–SNCG interactions	N-BubR1	K66, R67, N97, Q98, G99, K123, K135, E140 and R197	−1.00e+15	+9.10e+07	−1.00e+15
	SNCG	Q106, Q107, E108, E110, S112, K113, E114, K115, E116, E117, E120, S124 and D127			
ANK peptide–SNCG interactions	ANK peptide	G2, L6, H7, A9, L21, K1, A24, N27 and M30	−9.34e+14	+3.08e+06	−9.34e+14
	SNCG	Q106, Q107, E108, E110, S112, K113, E114, E117, E120, E121, S124 and D127			
Hsp70–SNCG interactions	HsP70	G25, Y49, S50, D51, N52, Q53, P54, R87, R151 and R153	−6.26e+14	+6.01e+07	−6.26e+14
	SNCG	E98, Q106, Q107, E110, K113, E116, E117,A122, S124 and D127			
Common residues of SNCG involved in all interactions		Q106, Q107, E108,E110, E114, E117, E120, and D127			

interaction with residues of the Hsp70-18kDa region. Among these residues, G126, E108, E98, R96 and S124 of SNCG form H-bonds with residues (A30, T47, A30, K41 and Q44) located in the peptide-binding site of 18kDHsp70. The above mentioned residues of SNCG can possibly be attributed to the initial interaction of SNCG with the substrate binding domain of Hsp70. Residues D127, E120, E110, Q106, E114, Q107, S124 and G125 of SNCG are thought to play a role in inducing the structural changes of Hsp70 that are essential for the interaction of Hsp70 with HOP protein to form a complex with Hsp90. The interacting conformation of 18kDHsp70-SNCG is presented in Fig. 6c. Based on these findings, we suggest that the C-terminal region of Hs-SNCG might interact with the 18kDa region of a nuclear free Hsp70 substrate binding domain. This interaction will enhance the binding affinity of Hsp70, resulting in the formation of a SNCG–Hsp70–HOP–Hsp90 complex. This complex can then bind to ER-α and gain the ability to bind estrogen, which will lead to the development of estrogen-dependent breast cancer. This mechanism is illustrated in Fig. 7. This finding provides a novel insight into the interacting mechanism of SNCG with Hsp70, and correlates with experimental identification of the interaction between 18kdHsp70 and the C-terminal tail region of SNCA.

Alanine scanning mutagenesis

From the interaction studies of SNCG with N-BubR1 and ANK peptide, the common residues of SNCG involved in interaction with both N-BubR1 and ANK peptide were identified (Q106, E107, E108, E110, E114, E117, E120 and D127). In order to confirm their role in mediating these interactions, alanine scanning mutagenesis was carried out by mutating these residues to alanine. The resulting models were built and used for docking studies with N-BubR1 and ANK peptides. Interestingly, interactions were not observed between N-BubR1and the mutated SNCG complex and the same was observed with ANK peptide and the mutated SNCG model. These findings confirm the strong interacting abilities of the above mentioned residues of SNCG. Furthermore, the same mutated model was docked with the substrate-binding domain of Hsp70 and the results confirm the strong protein–protein interacting ability of the above-mentioned residues of SNCG. From all these results, we suggest that Q106, E107, E108, E110, E114, E117, E120 and D127 are crucial residues of SNCG that play a strong role in its oncogenic function by mediating interaction with BubR1 and Hsp70 proteins.

Analysis of protein complex stability

The N-BubR1–SNCG, SNCG–ANK and SNCG–18kDHsp70 complexes were found to have energetically stable properties, as confirmed by MD studies carried out on these complexes using the GROMACS MD suite. After the MD studies, no changes were observed in the predicted hot spots. Moreover, the RMSD (Fig. 8) observed between the backbone atoms of the protein complexes obtained after the simulation studies revealed only very small deviations among them. The potential energy of the N-BubR1–SNCG complex was −36,517,328 $kJmol^{-1}$, −30,339,536 $kJmol^{-1}$ for the SNCG–ANK

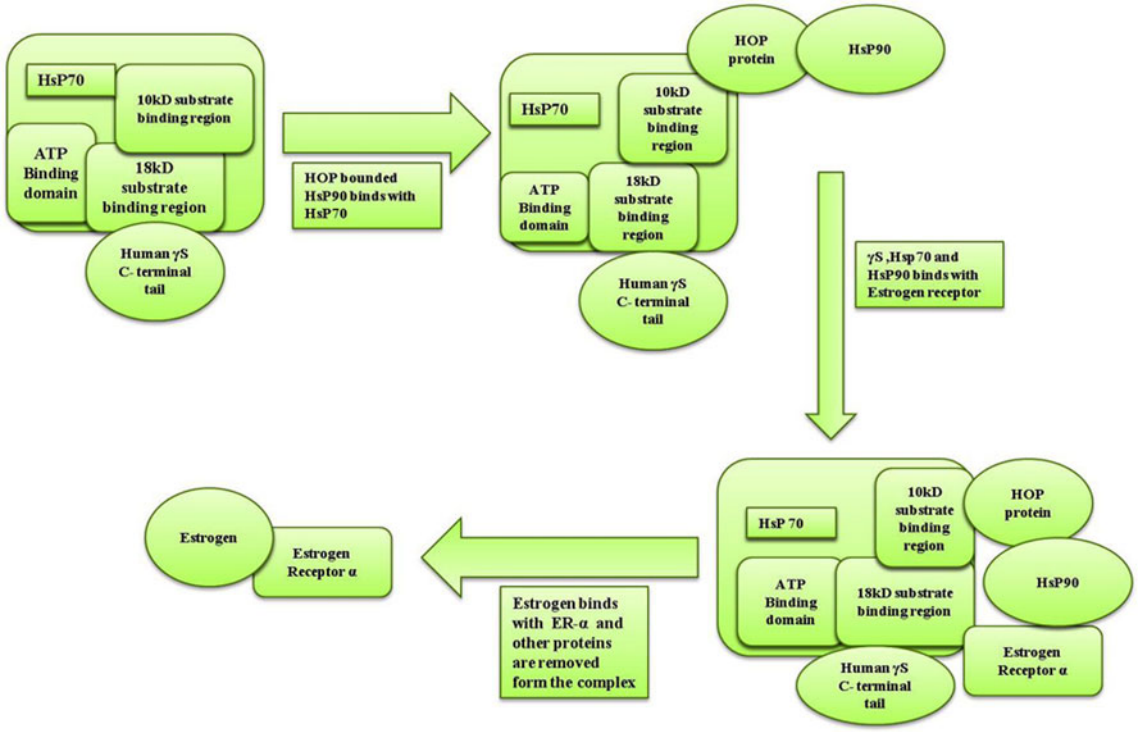

Fig. 7 Proposed mechanism of SNCG interaction with Hsp70, illustrating the formation of the following complexes: C-terminal tail region of SNCG–18kDHsp70, HOP–Hsp90–10kDa substrate binding region of Hsp70, SNCG–Hsp70–HOP–Hsp90–estrogen receptor-α

peptide complex and−47,888,355 kJmol^{-1} for the 18kDHsp70–SNCG complex. The maximum RMSD value observed in the case of N-BubR1–SNCG was about 0.60 nm, whereas it was 0.87 nm for SNCG–ANK and 0.83 nm for 18kDHsp70–SNCG. The N-BubR1–SNCG interaction leads to the inhibition of apoptosis of tumor cells, which clearly requires the stable interaction between these proteins; this stability was also reflected in our MD simulations, as was clearly evident from the results in which the complex is stabilized after 820 ps, with an RMSD value of about 0.5 nm. In contrast, the maximum RMSD value observed for SNCG–ANK and 18kDHsp70–SNCG interactions was 0.87 and 0.83 nm, respectively. These complexes were stabilized after 0.70 nm and 0.75 nm, respectively. After prolonged simulations, no changes were observed in the structure and in the interacting residues between N-BubR1 and SNCG. The same was observed in the other two cases. These results indicate that the interactions observed within these complexes are stable and the results are reliable.

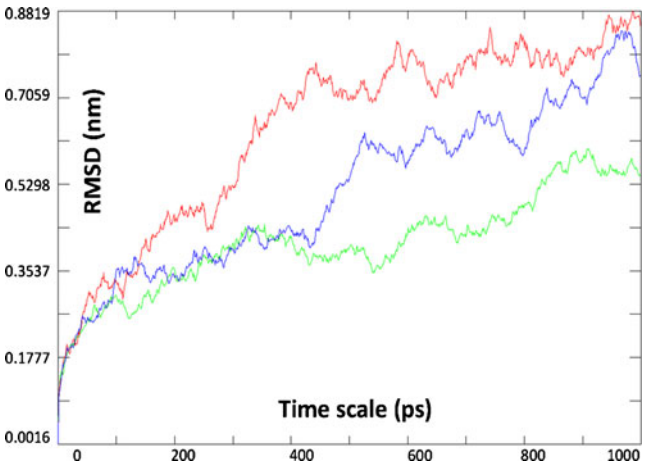

Fig. 8 Molecular dynamics (MD)-based analysis of the stability of protein–protein complexes: N-BubR1–SNCG, SNCG–ANK peptide and SNCG–18KdHsp70. Root mean square deviation (RMSD) of the backbone atoms with respect to the initial structure shows the stable nature of the protein–protein complexes. *Red* SNCG–ANK peptide, *blue* SNCG–18KdHsp70, *green* N-BubR1–SNCG. The plot was prepared using XY Plot windows version 4.1 [39]

Conclusions

Aberrant expression and interaction of SNCG with BubR1 and Hsp70 have been proven to mediate the development of breast cancer in human beings. Recently, a short ANK peptide designed synthetically was observed to form a complex with SNCG, inhibiting its ability to form a complex with BubR1. These findings confirm the strong oncogenic functions of SNCG, which have made it a crucial drug target in the treatment of breast and ovarian cancers. The disordered nature of SNCG was a potential challenging factor in its structure determination process and, moreover, the potential residues of SNCG that

mediate its oncogenic functions had not been identified. In an attempt to identify these residues, we predicted the structures of Hs-SNCG, BubR1-N-terminal region, 18kDa region of Hsp70 substrate binding domain and ANK peptides. These models were then used for protein–protein docking studies. Based on the interactions of SNCG with N-BubR1 and ANK peptide, the common residues of SNCG that mediate these interactions were identified. These residues of SNCG are predicted to play a strong oncogenic role by enabling interaction with N-BubR1, as was evident from the alanine scanning mutagenesis carried out on the SNCG model; these residues also involved in interaction with Hsp70. In addition, structural and function differences between Hs SNCG and SNCA were reported. Furthermore, we identified the sequence level relationship between Hs SNCG and Blinkin protein, a disordered protein that plays an important role in mediating the mitotic checkpoint activity of N-BubR1. Based on this result, we suggest that Hs-SNCG might mimic the structure of Blinkin in order to bind with N-BubR1. Also, SNCG was identified as the unique TPR motif binding protein, as was clear from its interaction with BubR1; no such interaction was observed with any other TPR motif containing protein. Finally, the unique ability of SNCG to interact only with the 18kDa region of Hsp70 substrate binding domain was reported for the first time through our studies. This finding correlates with experimental identification of the interaction of SNCA with the same region of Hsp70. All these results provide new insights into the interacting mechanism of Hs-SNCG, and could form the basis for new drug discovery approaches for treating breast and ovarian cancers.

Acknowledgments Research in the Laboratory of Structure Biology is supported by grants from University Grants Commission (UGC), Government of India, New Delhi, India. R.K. thanks the Centre for Bioinformatics, Pondicherry University, India.

References

1. Bruening W, Giasson BI, Klein-Szanto AJ, Lee VM, Trojanowski JQ, Godwin AK (2000) Synucleins are expressed in the majority of breast and ovarian carcinomas and in preneoplastic lesions of the ovary. Cancer 88(9):2154–2163
2. Lavedan C, Leroy E, Dehejia A, Buchholtz S, Dutra A, Nussbaum RL, Polymeropoulos MH (1998) Identification, localization and characterization of the human gamma-synuclein gene. Hum Genet 103(1):106–112
3. George JM (2002) The synucleins. Genome Biol 3(1): REVIEWS3002
4. Lavedan C (1998) The synuclein family. Genome Res 8(9):871–880
5. Gupta A, Godwin AK, Vanderveer L, Lu A, Liu J (2003) Hypomethylation of the synuclein gamma gene CpG island promotes its aberrant expression in breast carcinoma and ovarian carcinoma. Cancer Res 63(3):664–673
6. Pan ZZ, Bruening W, Giasson BI, Lee VM, Godwin AK (2002) Gamma-synuclein promotes cancer cell survival and inhibits stress-and chemotherapy drug-induced apoptosis by modulating MAPK pathways. J Biol Chem 277(38):35050–35060
7. Pan ZZ, Bruening W, Godwin AK (2006) Involvement of RHO GTPases and ERK in synuclein-gamma enhanced cancer cell motility. Int J Oncol 29(5):1201–1205
8. Davenport J, Harris LD, Goorha R (2006) Spindle checkpoint function requires Mad2-dependent Cdc20 binding to the Mad3 homology domain of BubR1. Exp Cell Res 312(10):1831–1842
9. Gupta A, Inaba S, Wong OK, Fang G, Liu J (2003) Breast cancer-specific gene 1 interacts with the mitotic checkpoint kinase BubR1. Oncogene 22(48):7593–7599
10. Hardwick KG, Johnston RC, Smith DL, Murray AW (2000) MAD3 encodes a novel component of the spindle checkpoint which interacts with Bub3p, Cdc20p, and Mad2p. J Cell Biol 148 (5):871–882
11. Zhou Y, Inaba S, Liu J (2006) Inhibition of synuclein-gamma expression increases the sensitivity of breast cancer cells to paclitaxel treatment. Int J Oncol 29(1):289–295
12. Singh VK, Zhou Y, Marsh JA, Uversky VN, Forman-Kay JD, Liu J, Jia Z (2007) Synuclein-gamma targeting peptide inhibitor that enhances sensitivity of breast cancer cells to antimicrotubule drugs. Cancer Res 67(2):626–633
13. Jiang Y, Liu YE, Goldberg ID, Shi YE (2004) Gamma synuclein, a novel heat-shock protein-associated chaperone, stimulates ligand-dependent estrogen receptor alpha signaling and mammary tumorigenesis. Cancer Res 64(13):4539–4546
14. Jiang Y, Liu YE, Lu A, Gupta A, Goldberg ID, Liu J, Shi YE (2003) Stimulation of estrogen receptor signaling by gamma synuclein. Cancer Res 63(14):3899–3903
15. Souza JM, Giasson BI, Lee VM, Ischiropoulos H (2000) Chaperone-like activity of synucleins. FEBS Lett 474(1):116–119
16. Roodveldt C, Bertoncini CW, Andersson A, van der Goot AT, Hsu ST, Fernandez-Montesinos R, de Jong J, van Ham TJ, Nollen EA, Pozo D, Christodoulou J, Dobson CM (2009) Chaperone proteostasis in Parkinson's disease: stabilization of the Hsp70/alpha-synuclein complex by Hip. EMBO J 28(23):3758–3770
17. Chappell TG, Konforti BB, Schmid SL, Rothman JE (1987) The ATPase core of a clathrin uncoating protein. J Biol Chem 262 (2):746–751
18. Cyr DM, Langer T, Douglas MG (1994) DnaJ-like proteins: molecular chaperones and specific regulators of Hsp70. Trends Biochem Sci 19(4):176–181
19. McGinnis S, Madden TL (2004) BLAST: at the core of a powerful and diverse set of sequence analysis tools. Nucleic Acids Res 32 (Web Server issue):W20–W25
20. Zhang Y (2008) I-TASSER server for protein 3D structure prediction. BMC Bioinform 9:40
21. Corpet F (1988) Multiple sequence alignment with hierarchical clustering. Nucleic Acids Res 16(22):10881–10890
22. Sali A, Blundell TL (1993) Comparative protein modelling by satisfaction of spatial restraints. J Mol Biol 234(3):779–815
23. Vriend G (1990) WHAT IF: a molecular modeling and drug design program. J Mol Graph 8(1):52–56, 29
24. Lovell SC, Davis IW, Arendall WB 3rd, de Bakker PI, Word JM, Prisant MG, Richardson JS, Richardson DC (2003) Structure validation by Calpha geometry: phi, psi and Cbeta deviation. Proteins 50(3):437–450
25. Colovos C, Yeates TO (1993) Verification of protein structures: patterns of non bonded atomic interactions. Protein Sci 2(9):1511–1519

26. Liang J, Edelsbrunner H, Woodward C (1998) Anatomy of protein pockets and cavities: measurement of binding site geometry and implications for ligand design. Protein Sci 7(9):1884–1897
27. Lee B, Richards FM (1971) The interpretation of protein structures: estimation of static accessibility. J Mol Biol 55(3):379–400
28. Rocchia W, Sridharan S, Nicholls A, Alexov E, Chiabrera A, Honig B (2002) Rapid grid-based construction of the molecular surface and the use of induced surface charge to calculate reaction field energies: applications to the molecular systems and geometric objects. J Comput Chem 23(1):128–137
29. Dominguez C, Boelens R, Bonvin AM (2003) HADDOCK: a protein-protein docking approach based on biochemical or biophysical information. J Am Chem Soc 125(7):1731–1737
30. Huey R, Morris GM, Olson AJ, Goodsell DS (2007) A semiempirical free energy force field with charge-based desolvation. J Comput Chem 28(6):1145–1152
31. Shen MY, Sali A (2006) Statistical potential for assessment and prediction of protein structures. Protein Sci 15(11):2507–2524
32. Van der Spoel D, Lindahl E, Hess B, Groenhof G, Mark AE, Berendsen HJ (2005) GROMACS: fast, flexible, and free. J Comput Chem 26(16):1701–1718
33. Ulmer TS, Bax A, Cole NB, Nussbaum RL (2005) Structure and dynamics of micelle-bound human alpha-synuclein. J Biol Chem 280(10):9595–9603
34. Bolanos-Garcia VM, Kiyomitsu T, D'Arcy S, Chirgadze DY, Grossmann JG, Matak-Vinkovic D, Venkitaraman AR, Yanagida M, Robinson CV, Blundell TL (2009) The crystal structure of the N-terminal region of BUB1 provides insight into the mechanism of BUB1 recruitment to kinetochores. Structure 17 (1):105–116
35. Kohl A, Binz HK, Forrer P, Stumpp MT, Pluckthun A, Grutter MG (2003) Designed to be stable: crystal structure of a consensus ankyrin repeat protein. Proc Natl Acad Sci USA 100(4):1700–1705
36. Morshauser RC, Hu W, Wang H, Pang Y, Flynn GC, Zuiderweg ER (1999) High-resolution solution structure of the 18 kDa substrate-binding domain of the mammalian chaperone protein Hsc70. J Mol Biol 289(5):1387–1403
37. Thompson JD, Gibson TJ, Higgins DG (2003) Multiple sequence alignment using ClustalW and ClustalX. In: Baxevanis AD (ed) Current Protocols in Bioinformatics. Wiley, San Francisco, pp 2.3.1–2.3.22
38. DeLano WL (2002) The PyMOL Molecular Graphics System. DeLano Scientific LLC, San Carlos, CA. http://www.pymol.org
39. Krishna M, John K, Helen K, Bryan F (1994) XYPLOT-Data Analysis Program, Creative Consulting for Research & Education. http://ccreweb.org/software/xyplot/xyplot.html